



Sympathetic Nervous Regulation of Calcium and Action Potential Alternans in the Intact Heart

James Winter^{1,2*}, Martin J. Bishop³, Catherine D. E. Wilder¹, Christopher O'Shea², Davor Pavlovic² and Michael J. Shattock¹

¹ School of Cardiovascular Medicine and Sciences, King's College London, United Kingdom, ² Institute of Cardiovascular Sciences, College of Medicine and Dental Sciences, University of Birmingham, United Kingdom, ³ Biomedical Engineering Department, King's College London, United Kingdom

OPEN ACCESS

Edited by:

Tobias Opthof,
Academic Medical Center (AMC),
Netherlands

Reviewed by:

Alessandro Capucci,
Università Politecnica delle Marche,
Italy
Jong-Kook Lee,
Osaka University, Japan

*Correspondence:

James Winter
james.winter@kcl.ac.uk

Specialty section:

This article was submitted to
Cardiac Electrophysiology,
a section of the journal
Frontiers in Physiology

Received: 27 September 2017

Accepted: 08 January 2018

Published: 23 January 2018

Citation:

Winter J, Bishop MJ, Wilder CDE, O'Shea C, Pavlovic D and Shattock MJ (2018) Sympathetic Nervous Regulation of Calcium and Action Potential Alternans in the Intact Heart. *Front. Physiol.* 9:16. doi: 10.3389/fphys.2018.00016

Rationale: Arrhythmogenic cardiac alternans are thought to be an important determinant for the initiation of ventricular fibrillation. There is limited information on the effects of sympathetic nerve stimulation (SNS) on alternans in the intact heart and the conclusions of existing studies, focused on investigating electrical alternans, are conflicted. Meanwhile, several lines of evidence implicate instabilities in Ca handling, not electrical restitution, as the primary mechanism underpinning alternans. Despite this, there have been no studies on Ca alternans and SNS in the intact heart. The present study sought to address this, by application of voltage and Ca optical mapping for the simultaneous study of APD and Ca alternans in the intact guinea pig heart during direct SNS.

Objective: To determine the effects of SNS on APD and Ca alternans in the intact guinea pig heart and to examine the mechanism(s) by which the effects of SNS are mediated.

Methods and Results: Studies utilized simultaneous voltage and Ca optical mapping in isolated guinea pig hearts with intact innervation. Alternans were induced using a rapid dynamic pacing protocol. SNS was associated with rate-independent shortening of action potential duration (APD) and the suppression of APD and Ca alternans, as indicated by a shift in the alternans threshold to faster pacing rates. Qualitatively similar results were observed with exogenous noradrenaline perfusion. In contrast with previous reports, both SNS and noradrenaline acted to flatten the slope of the electrical restitution curve. Pharmacological block of the slow delayed rectifying potassium current (I_{Ks}), sufficient to abolish I_{Ks} -mediated APD-adaptation, partially reversed the effects of SNS on pacing-induced alternans. Treatment with cyclopiazonic acid, an inhibitor of the sarco(endo)plasmic reticulum ATPase, had opposite effects to that of SNS, acting to increase susceptibility to alternans, and suggesting that accelerated Ca reuptake into the sarcoplasmic reticulum is a major mechanism by which SNS suppresses alternans in the guinea pig heart.

Conclusions SNS suppresses calcium and action potential alternans in the intact guinea pig heart by an action mediated through accelerated Ca handling and via increased I_{Ks} .

Keywords: alternans, ventricular fibrillation, sympathetic nervous system, calcium transient, action potential duration, sarco(endo)plasmic reticulum ATPase, intact heart, optical mapping

INTRODUCTION

Beat-to-beat oscillations in action potential duration (APD), termed APD alternans, are thought to be an important determinant of the induction of ventricular fibrillation (VF), by acting to promote functional conduction block and wave-break (Weiss et al., 2011). Mechanistically, APD alternans have been proposed to arise either as a function of the steepness of the electrical restitution or as secondary events driven by beat-to-beat oscillations in the amplitude of the intracellular Ca transient (Nolasco and Dahlen, 1968; Díaz et al., 2004).

It is known that APD and Ca alternans are affected by the sympathetic nervous system via β -adrenoceptor dependent signaling pathways. Sympathetic nerve stimulation (SNS) is reported to suppress electrical (T-wave) and mechanical alternans associated with rapid atrial pacing in the canine heart (Euler et al., 1996). Similarly, β -adrenoceptor agonists are reported to suppress Ca transient alternans in isolated myocytes (Hüser et al., 2000; Florea and Blatter, 2012). However, studies in isolated rabbit hearts suggest that SNS promotes alternans by acting to steepen the slope of the electrical restitution curve (Ng et al., 2007).

Adrenergic stimulation exerts multiple effects on Ca handling and cardiac electrophysiology, including, an increase in the magnitude of the inward L-type Ca current, augmentation in the amplitude of the intracellular Ca transient, the acceleration of Ca uptake through the sarco/endoplasmic reticulum Ca^{2+} -ATPase (SERCA) and increased conductance of the slow delayed rectifying K current (I_{Ks})—all of which could modulate Ca and APD alternans (Bers, 2002). Studies to date have largely focussed on the effects of adrenergic stimulation on Ca transient alternans in isolated myocytes treated with sympathomimetic agents, e.g., isoproterenol. Less is known about how activation of the regionally heterogeneous sympathetic innervation influences APD and Ca alternans in the intact heart with preserved cell-to-cell coupling, regional differences in ion channel expression and Ca handling properties. Currently, there are only two experimental reports examining the effects of SNS on alternans in the intact heart, which offer opposing conclusions (Euler et al., 1996; Ng et al., 2007). Reports in the rabbit, suggesting that SNS promotes alternans by steepening the slope of the electrical restitution curve, appear conflicted with more recent mechanistic insights from single cells, which place greater focus on instabilities of Ca handling. However, to date, there have been no studies of SNS on Ca alternans in the intact heart. The present study sought to address the hypothesis that SNS would act to suppress alternans. Experiments utilized voltage and Ca optical mapping for the simultaneous study of APD and Ca alternans in the intact guinea pig heart during electrical stimulation of the sympathetic nerves.

Abbreviations: APD, action potential duration; SERCA, sarco(endoplasmic reticulum ATPase; SR, sarcoplasmic reticulum; SNS, sympathetic nerve stimulation.

MATERIALS AND METHODS

Animal Welfare

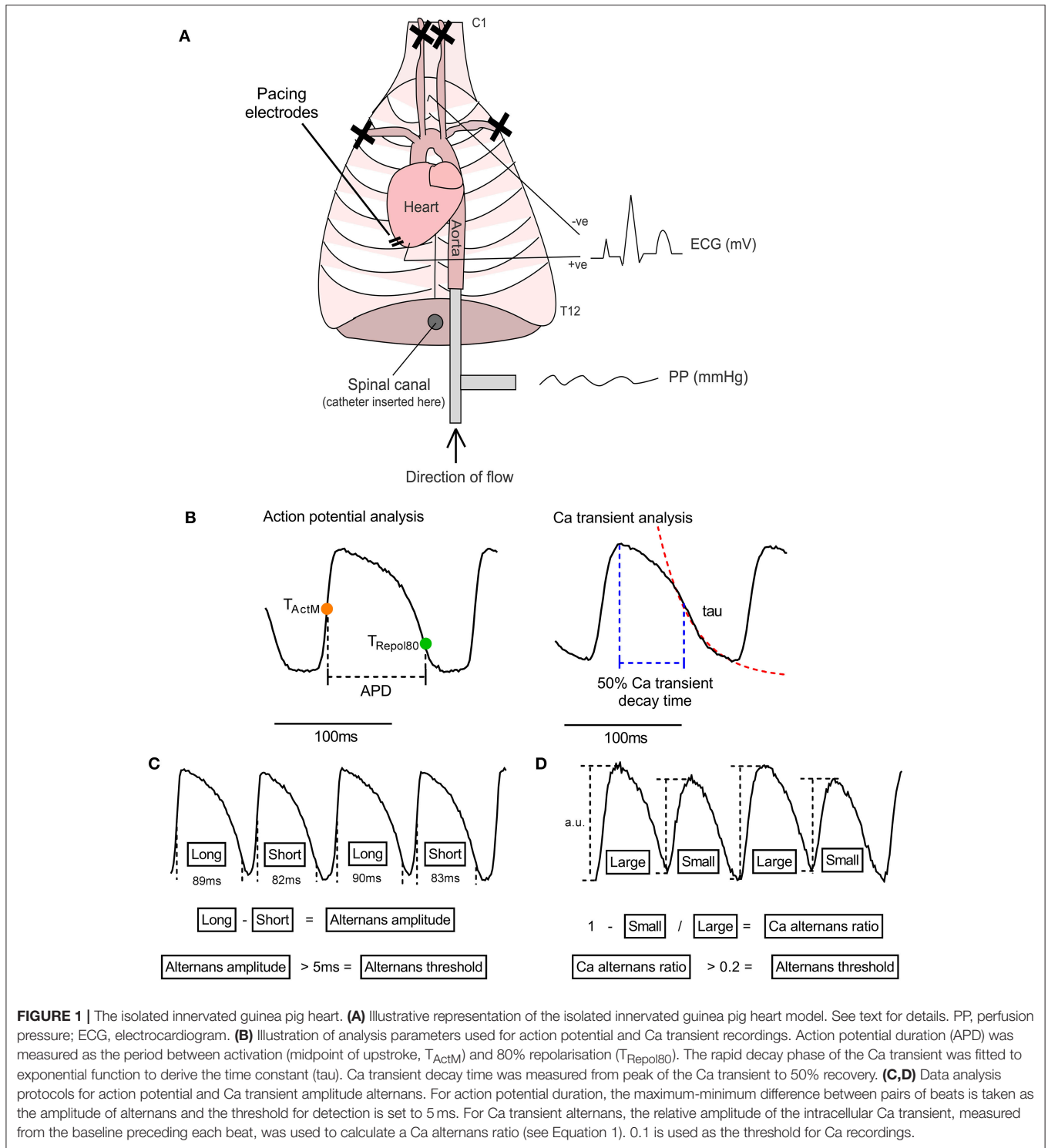
All procedures were undertaken in accordance with ethical guidelines set out by the UK Animals (Scientific Procedures) Act 1986 and Directive 2010/63/EU of the European Parliament on the protection of animals used for scientific purposes. Studies conformed to the Guide for the Care and Use of Laboratory Animals published by the U.S. National Institutes of Health under assurance number A5634-01. Studies were approved by the King's College London Animal Welfare and Ethical Review Board.

Isolated Innervated Guinea Pig Heart and Nerve Stimulation

Experiments were performed in adult male guinea pigs (400–650 g) utilizing an adaptation of the innervated rabbit heart preparation first described by Ng et al. (2001) (see **Figure 1A**). Animals were anesthetized (sodium pentobarbitone, 160 mg/kg i.p.), an incision was made below the diaphragm and the rib cage was resected on both sides. The descending aorta was isolated and cannulated, and the heart retrograde perfused with ice-cold oxygenated buffer (see below). The subclavian and carotid vessels were ligated, the heart and thorax isolated between cervical vertebrae 1 and thoracic vertebrae 12 and the preparation was transferred to a perfusion rig. Hearts were perfused in Langendorff mode through the descending aorta (perfusion pressure 65–75 mmHg, 37°C). Buffer solutions contained (in mmol/L): NaCl 114, KCl 4, CaCl 1.6, NaHCO_3 24, MgSO_4 1, NaH_2PO_4 1.1, glucose 11.0, sodium pyruvate 1.0 and decamethonium bromide 0.01. Solutions were filtered using an in-line cellulose filter (5 μm pore diameter). An electrocardiogram (ECG) was recorded throughout the experiment (PowerLab 16/35 + Octal Bioamp, ADInstruments, Australia). Bi-lateral stimulation of efferent sympathetic nerves was conducted by insertion of a decapolar 5-french electrophysiological catheter into the spinal column, which was advanced to the level of the 5–7th cervical vertebrae. The distal poles of the catheter were attached to a constant voltage stimulator set at 40 V and with pulse duration of 2 ms (DS2A, Digitimer, UK). At the beginning of each experiment the response to nerve stimulation was tested and the frequency of electrical stimulation was varied (range 3–8 Hz) to give a steady state heart rate of between 320 and 340 bpm. Therein, parameters were kept constant during all experimental protocols and were stable for the duration of the experiment.

Optical Mapping

Hearts were uncoupled with blebbistatin (15 $\mu\text{mol/L}$) and stained with either di-8-anepbs (1 mg/ml in DMSO; 200–300 μL), rh-237 (2.5 mg/ml in DMSO; 25–50 μL) or a combination of rh-237 (as previous) and rhod-2 AM (200 μg dissolved in 200 μL DMSO + 20 μL 20% pluronic F-127). Dyes were injected slowly into the perfusion line over a 5 to 10-min period. Excitation light was at 530 ± 25 nm, with emission light collected at >610 nm for di-8-anepbs, >710 nm for rh-237 and 585 ± 20 nm for rhod-2. Hearts were imaged through an Olympus MVX10



stereomicroscope and signals recorded on Evolve Delta 512 × 512 pixel EMCCD cameras (500 Hz sampling rate, 64 × 64 pixels, 355 micron/pixel). Where appropriate, HMR 1556 (2 μmol/L in DMSO) and cyclopiazonic acid (CPA, 10 μmol/L in DMSO) were added directly to the perfusate and allowed to equilibrate for 10-min. Final DMSO concentration was <0.001% in all experiments.

In some studies, noradrenaline (200 nmol/L) + ascorbic acid (50 μmol/L) was added directly to the perfusate.

Pacing and VF Induction

Hearts were paced from the left ventricular epicardial apex through silver bipolar pacing wires using a constant current

stimulator (DS3, Digitimer, UK). Pulse duration and pulse amplitude were fixed at 2 ms and 5 mA, respectively. Initial studies utilized a dynamic pacing protocol in which hearts were paced at a cycle length for 100 beats and cycle length was then reduced in 10 ms steps every 10 beats until VF was induced or 2:1 block occurred. This pacing protocol was selected to limit extended periods of nerve stimulation, which lasted approximately 5-min per protocol. Where necessary, after VF induction, hearts were cardioverted by injection of high K⁺ solution (100 mmol/L) into the perfusion line. Hearts were allowed to recover for a minimum of 5-min between subsequent pacing protocols, or until heart rate and ECG parameters had stabilized. Due to substantive action potential prolongation, during HMR 1556 perfusion the dynamic pacing protocol was started from an initial pacing rate of 220 ms.

In some studies, the effects of noradrenaline on the Ca transient amplitude restitution relationship were measured using an extra-stimulus (S1–S2) pacing protocol, consisting of a 20-beat S1 train (cycle length = 200 ms) and a single S2 delivered at progressively shorter coupling intervals until loss of ventricular capture (10 ms step reduction from 200 ms). Ca transient restitution was measured as the % change in amplitude relative to the last S1 beat.

Data Analysis

Analysis was performed using custom MatLab scripts (MatLab, r2017b, MathWorks, USA). Data were processed with a Gaussian spatial filter (sigma = 1.5) and 5th order Savitzky-Golay temporal filter. Activation time was defined as the midpoint of the action potential upstroke. Repolarisation times were taken at 80% recovery to the resting membrane potential, measured from the peak to the end of the action potential. APD was taken as the difference between activation and repolarisation times (see **Figure 1B**).

APD alternans amplitude was calculated as the max-min for each pair of beats. A Ca alternans ratio was calculated from the difference in amplitude between large (and small Ca transients, according to Equation 1 (as per Wu and Clusin, 1997)). An illustration of the analysis procedure for APD and Ca transient alternans can be found in **Figures 1C,D**.

$$\text{Ca alternans ratio} = 1 - \text{small}/\text{large} \quad (1)$$

An alternans threshold of 5 ms and 0.1 was used for APD and Ca alternans, respectively.

APD and Ca transient restitution curves were fitted to Equation 2, where APD_{ss} is the APD at the slowest pacing rate, τ is the time constant, DI is the diastolic interval and b is the normalized minimum APD.

$$APD = APD_{ss}^* [1 - b^* \exp(-DI/\tau)] \quad (2)$$

Presented data represent mean \pm SEM. Statistical comparisons were made by paired Student's *t*-test and two-way repeated

measures ANOVA, with Tukey's *post-hoc* tests, as defined in the figure legends.

RESULTS

The Transition from Concordant to Discordant APD Alternans Underpins VF Induction during Dynamic Pacing

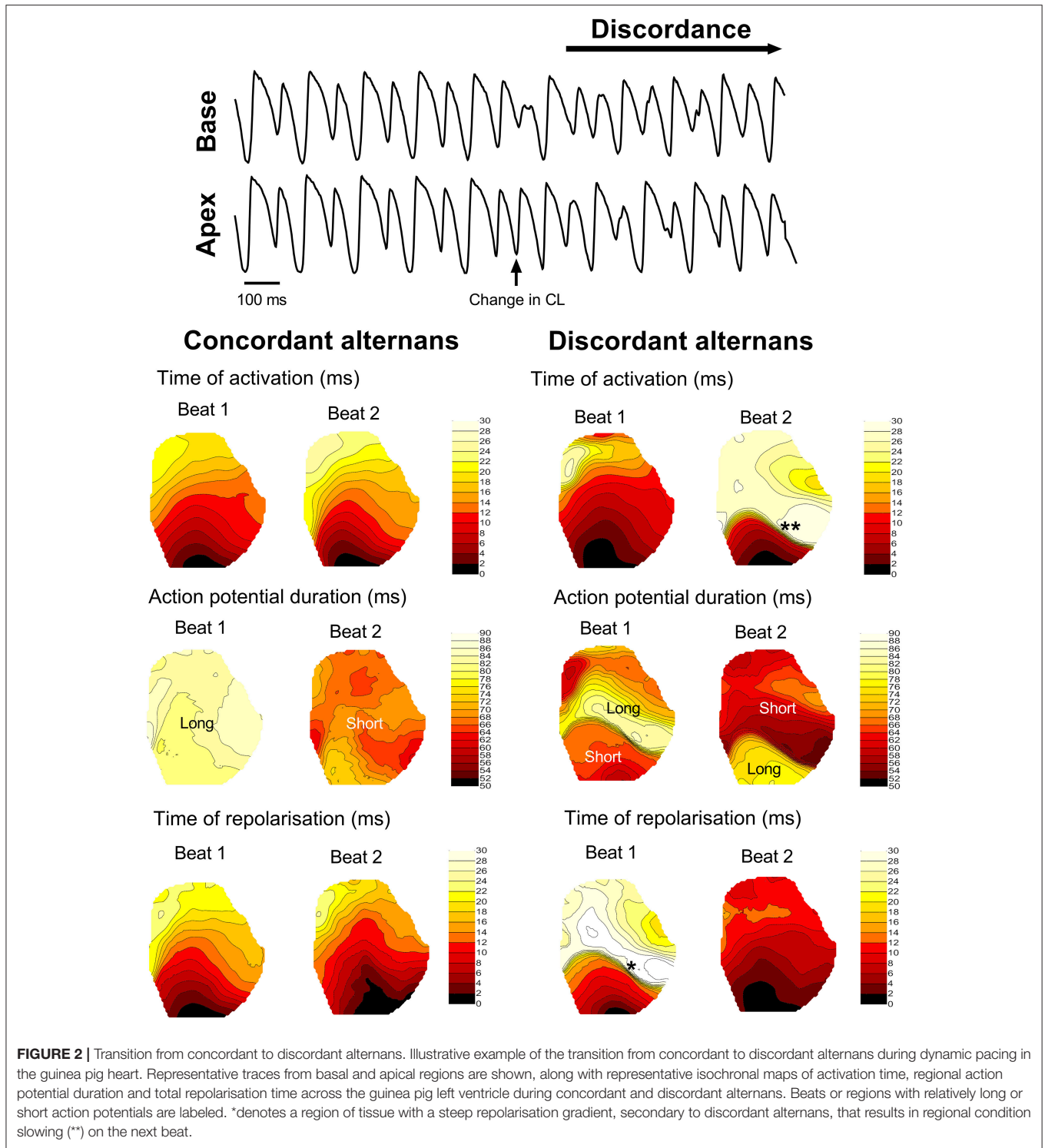
Dynamic (incremental) rapid-pacing of the guinea pig left ventricle was associated with oscillations in APD, which exhibited a pattern of long-short-long-short on a beat-to-beat basis. Alternans were initially spatially concordant (i.e., in-phase) across the ventricular surface, with a magnitude that increased as a function of pacing rate (left-hand side of **Figure 2**). With further increases in rate, spatially concordant alternans transitioned to become spatially discordant, where different regions of the ventricular myocardium exhibited counter-phase oscillations in APD (right-hand side of **Figure 2**), which was attributed to functional conduction slowing in regions with steep regional repolarisation gradients (see **Figure 2**). At a critical pacing rate, the resulting local differences in tissue repolarisation times (i.e., refractoriness), resulted in lines of unidirectional functional conduction block, retrograde activation, and the initiation of sustained re-entry/VF.

SNS Suppresses Cardiac Alternans in the Guinea Pig Heart

Data presented in **Figure 3** illustrate the effects of sustained SNS on dynamic pacing-induced APD and Ca transient alternans in the isolated innervated guinea pig heart. Stimulation of efferent sympathetic nerves resulted in rate-independent shortening of ventricular APD (**Figures 3A,B**) and the acceleration of Ca transient decay (i.e., decrease in tau; **Figures 3E,F**). Concomitant with these changes was the suppression of electrical and Ca alternans, as indicated by a leftward shift in the alternans cycle length relationships (**Figures 3C,G**) and a decrease in the alternans threshold (**Figures 3D,H**). Example recordings of rapid pacing induced APD and Ca transient alternans in the absence and presence of SNS are shown in **Figures 3C,G**, respectively. Addition of exogenous noradrenaline (200 nmol/L) to the perfusion buffer exerted qualitatively similar effects to those of SNS, acting to suppress APD alternans (**Figure 4**).

SNS Flattens the Slope of the Electrical Restitution Curve

Previous reports suggest that SNS acts to steepen the electrical restitution curve, and by this mechanism, augments pacing-induced APD alternans (Ng et al., 2007). However, this conflicts with our recent findings (Shattock et al., 2017), as we would predict that shortening of the ventricular action potential, would act to flatten, not steepen, the slope of the electrical restitution curve. To address this issue, we examined APD rate-adaptation with and without SNS. Data are presented in **Figure 5**. In accord with our previous observations, SNS and noradrenaline was associated with the flattening of the dynamic electrical

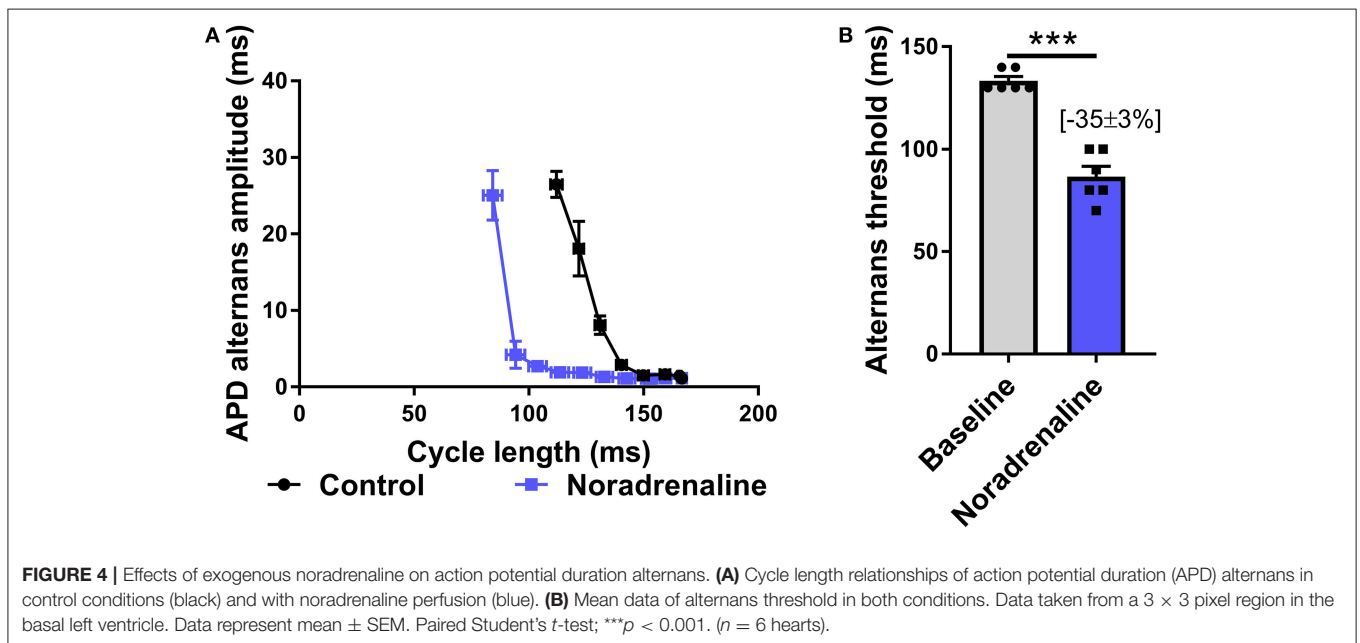
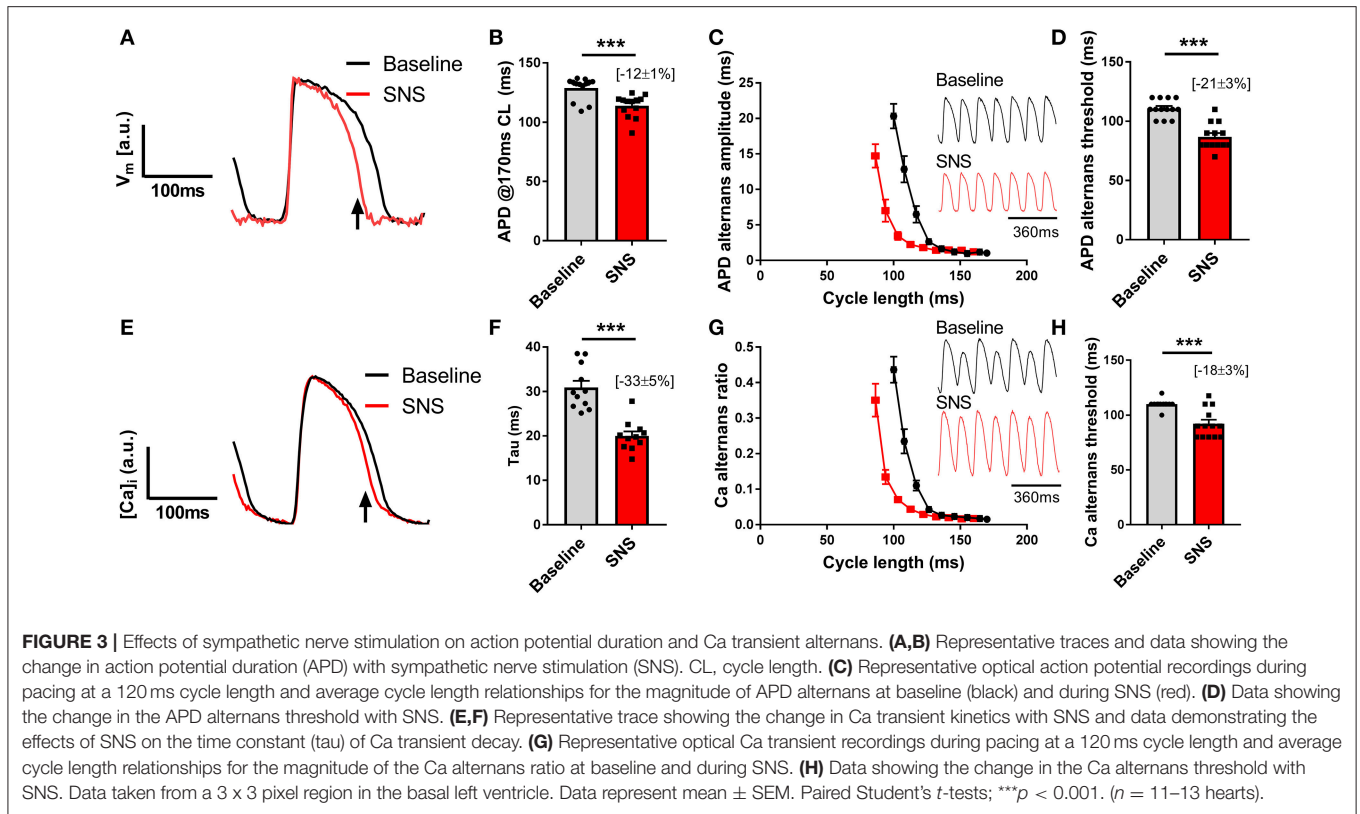


restitution curve, secondary to shortening of the ventricular APD (Figures 5A,C). By normalizing the slope of the curves as a function of the APD at steady-state (i.e., the longest pacing cycle length) difference in slopes between conditions was abolished (Figures 5B,C).

Mechanism(s) of Action of SNS Modulation of Cardiac Alternans

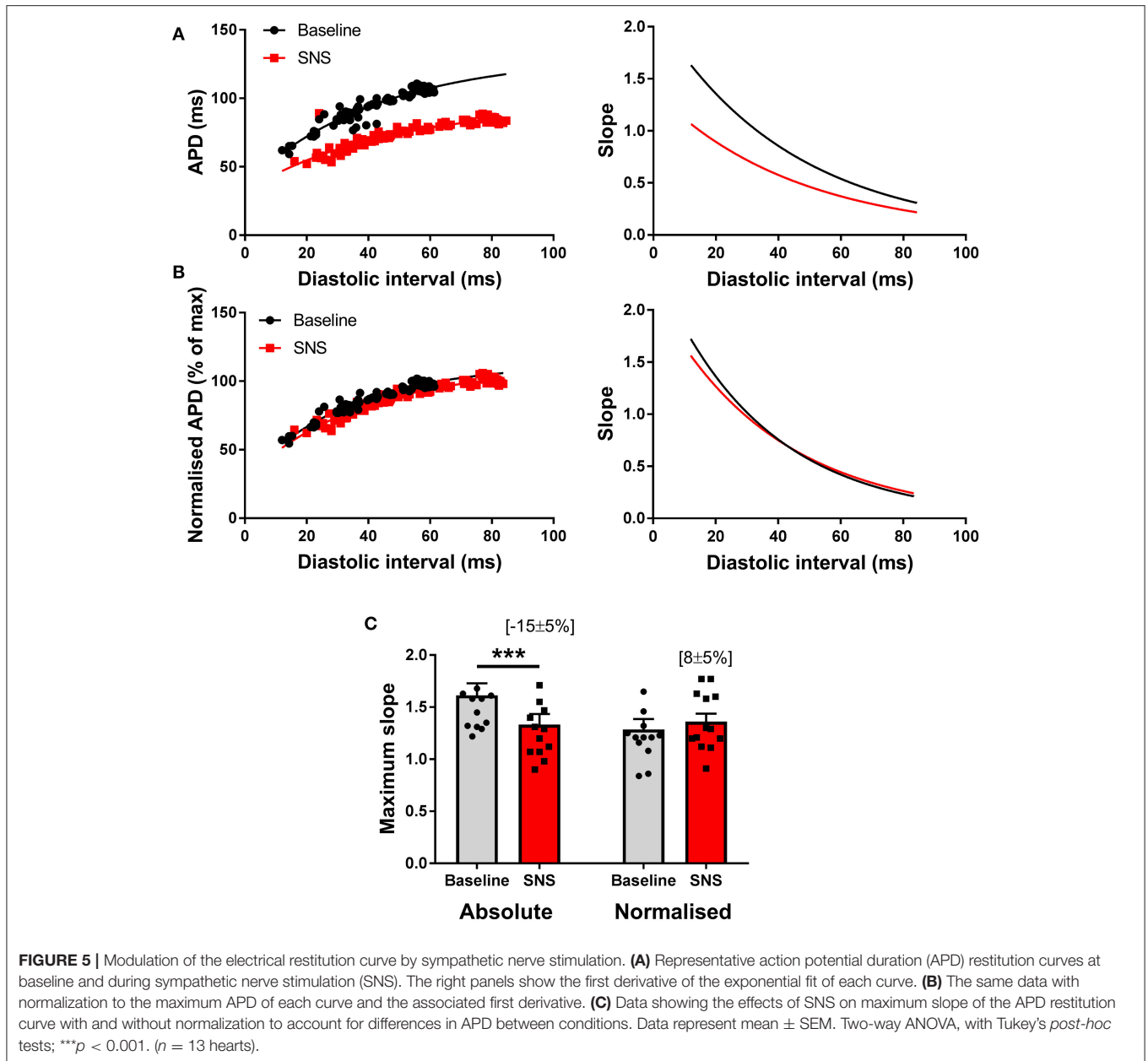
Role of APD Adaptation

Augmentation of I_{Ks} is responsible for the rate-independent shortening of ventricular APD observed during adrenergic



stimulation. By use of a selective inhibitor (HMR 1556, 2 μmol/L), we investigated the role of I_{Ks} in the effects of SNS. Data are presented in **Figure 6**. I_{Ks} block caused substantive prolongation of ventricular APD and prevented adaptation of the action potential during nerve stimulation (**Figures 6A–C**). HMR

1556 shifted the alternans cycle length relationship to the right, so that the threshold for alternans occurred at significantly slower pacing rates compared with control conditions (**Figure 6D**). In the presence of HMR 1556, SNS still suppressed alternans, however, the magnitude decrease in the alternans threshold was

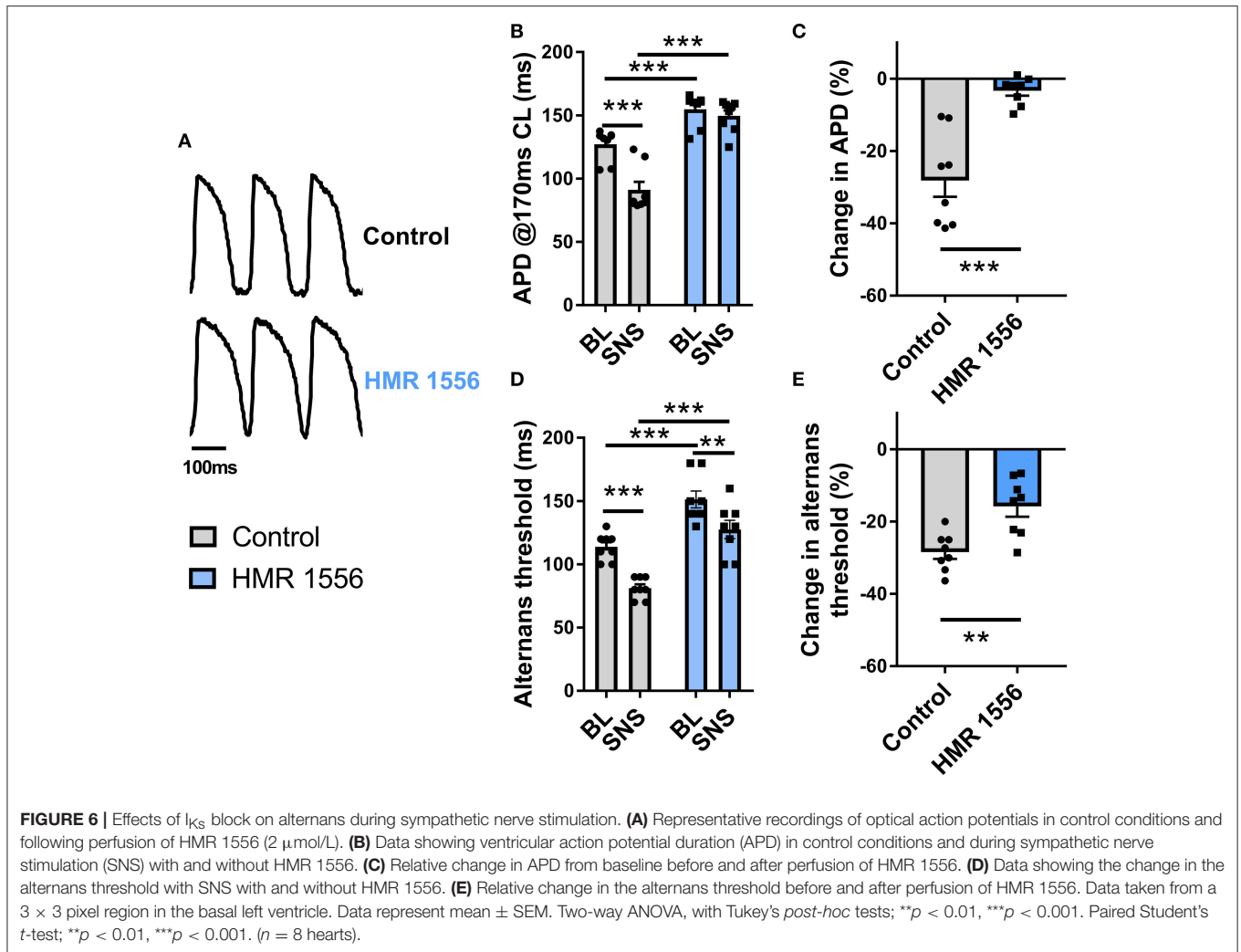


less compared with control measurements ($\sim 50\%$ reduction in response to SNS; **Figure 6E**). This indicates that I_{K_s} -mediated shortening of the ventricular action potential plays an important role in the suppression of cardiac alternans by SNS.

Role of Ca Handling

As shown in **Figure 3**, SNS accelerates the rate of decay of the intracellular Ca transient, which is indicative of enhanced Ca reuptake via SERCA, a major target of adrenergic signaling pathways. In **Figure 7A**, it is shown that noradrenaline (equivalent to the action of SNS) causes a leftward shift in the Ca transient S1S2 (extra-stimulus) restitution relationship; an observation which is consistent with the notion that Ca

alternans are a function of the rate of Ca extrusion from the cytosol (see Discussion). During SNS, Ca uptake into the SR is accelerated, and so the amplitude of the Ca transient is preserved over a broader range of pacing rates (**Figure 7A**). Alternans arise when the rate of SR Ca recovery cannot keep up with the underlying beating rate. Thus, the threshold for alternans occurs at faster rates (i.e., shorter cycle lengths) during adrenergic stimulation (**Figures 3G,H**). In support of this argument, we found that perfusion of a submaximal concentration of the CPA ($10 \mu\text{M}$), an inhibitor of SERCA, exerted opposite effects to those observed with SNS. Perfusion of CPA was associated with slowing of the decay of the intracellular Ca transient (**Figures 7B,C**), prolongation of the ventricular action potential (**Figure 7D**) and



a rightward shift in the cycle length relationship for both APD and Ca alternans (Figures 7E,F). Notably, the suppression of alternans by SNS was preserved in the presence of CPA (data not shown), but this was predicted, as adrenergic stimulation affects the K_m of SERCA, whereas CPA inhibits the pump (i.e., reduces pump density). Thus, SNS would still be expected to accelerate Ca uptake in the presence of submaximal concentrations of CPA.

In summary, both enhanced rates of cytosolic Ca extrusion and shortening of the ventricular action potential, via increased I_{Ks} , contribute to the suppression of cardiac alternans by SNS.

DISCUSSION

The results of the present study indicate that SNS suppresses APD and Ca alternans in the intact guinea pig heart. SNS acts to shift the threshold for alternans to a lower set point, so that faster beating rates are required to induce instabilities of Ca cycling and membrane potential. Our observations are

confirmatory of previous studies in isolated myocytes treated with sympathomimetic agents (Hüser et al., 2000; Florea and Blatter, 2012), as well as indirect observations in the dog (i.e., mechanical and T-wave alternans) (Euler et al., 1996), but differ from the reported effects of SNS in the rabbit heart (i.e., augmented APD alternans secondary to steepening of the electrical restitution curve). The results of the present study suggest that in the guinea pig heart, SNS suppresses alternans by two main mechanisms of action; (1) accelerated reuptake of cytosolic Ca into the SR and (2) I_{Ks} -mediated shortening of the ventricular action potential. In this paradigm, Ca-dependent mechanisms are the major driver of alternans, whilst the slope of the restitution curve plays a smaller modulatory role.

Cellular Mechanisms of Alternans and Modulation by Adrenergic Stimulation

Cardiac alternans have received substantial experimental and clinical interest due to the strong association between alternans, cardiac pathology, and sudden death. Understanding of the

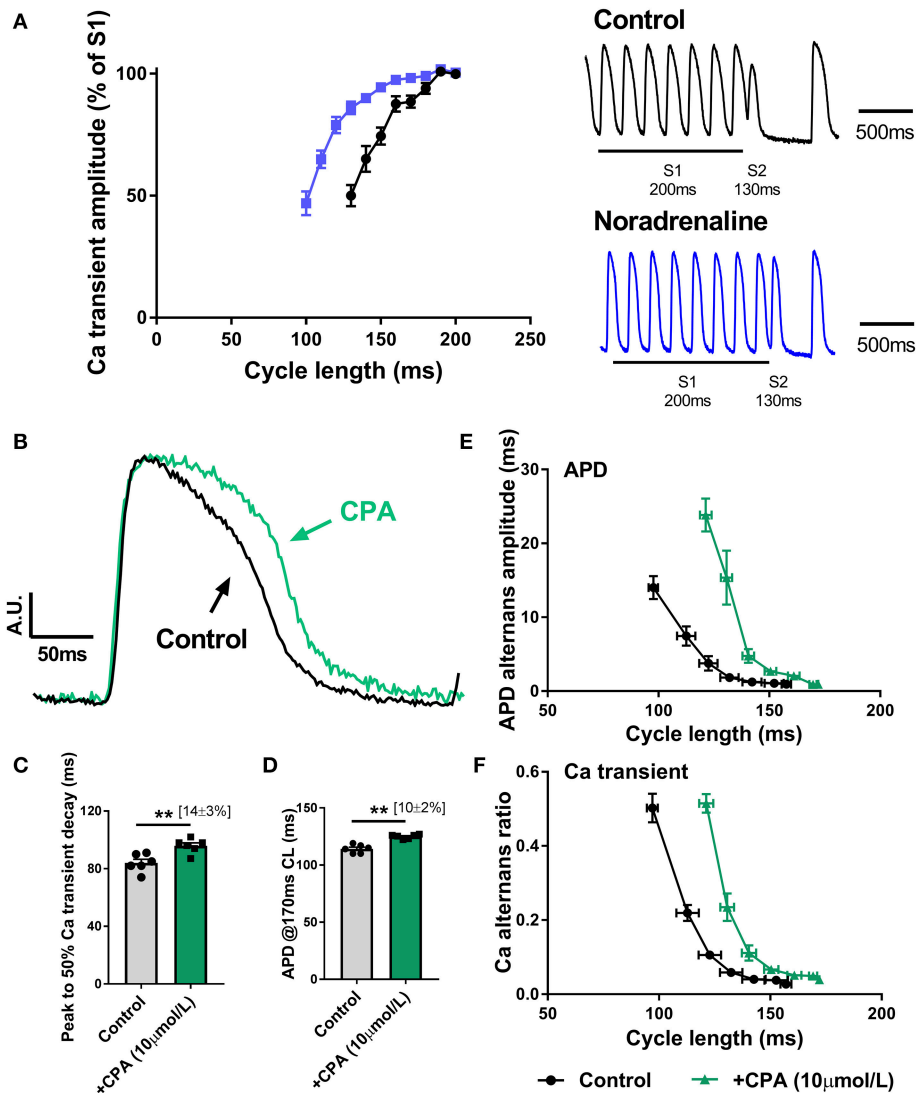


FIGURE 7 | Role of altered Ca handling in the action of sympathetic nerve stimulation on cardiac alternans **(A)** S1S2 (extra-stimulus) Ca transient amplitude restitution relationships in the presence and absence of noradrenaline (200 nmol/L). Inset are representative traces of a single extra-stimulus (S2) at a 130 ms cycle length in the absence and presence of noradrenaline. **(B)** Amplitude-normalized intracellular Ca transients recorded in control conditions and with cyclopiazonic acid (CPA, 10 μ mol/L). **(C,D)** Data on the effects of CPA on action potential duration (APD) and the time to 50% decay of the intracellular Ca transient. **(E,F)** Data on the cycle length relationships for APD and Ca amplitude alternans. Data taken from a 3×3 pixel region in the basal left ventricle. Paired Student's *t*-test; ** $p < 0.01$. Data are mean \pm SEM. ($n = 5$ –6 hearts).

mechanistic basis for alternans has evolved from an initial focus on voltage-dependent mechanisms (i.e., the slope of the electrical restitution curve), toward the more recent recognition of Ca cycling instabilities as the primary driving mechanism (Weiss et al., 2011). In what is now a classical study, Diaz et al. first proposed that the steep Ca load-release relationship of the sarcoplasmic reticulum was the primary basis of Ca (and, indirectly, APD) alternans (Díaz et al., 2004). However, this idea was subsequently challenged by observations that Ca transient alternans can occur in the absence of oscillations in the diastolic Ca level of the SR (Picht et al., 2006). It has since been proposed that Ca transient alternans are a function

of the recovery from inactivation of the RyRs, which have an intrinsic refractory period that is modulated by cytosolic and luminal Ca levels (Picht et al., 2006; Shkryl et al., 2012; Wang et al., 2014; Qu et al., 2016). Recent theoretical modeling based on the emergent properties of the cardiac couplon network, indicates that the key factors responsible for alternans are the random nature of Ca sparks (RyR openings), RyR refractoriness and recruitment of neighboring Ca-release units (the 3R theory) (Weiss et al., 2011; Qu et al., 2016). In this paradigm, the steep load-release relationship arises intrinsically from the myocyte couplon network, as recently proposed by Qu et al. (2016). Thus, Ca transient alternans involve several

interacting and interdependent mechanisms. For example, in studies of SR Ca cycling in isolated rabbit hearts, Wang et al. reported that alternans of SR Ca-release precede changes in diastolic SR Ca (Wang et al., 2014). However, at faster pacing rates, diastolic SR Ca oscillates on a beat-by-beat basis. This suggests that RyR refractoriness is the principal driver of Ca transient alternans, but at faster rates, the steep load-release relationship of the SR is engaged. Thus, the study of Wang et al. appears to be in keeping with the unified model of Qu et al. (2016).

In the present study, we report two major mechanisms of action for the sympathetic nervous modulation of cardiac alternans; (1) enhanced cytosolic Ca extrusion and (2) I_{Ks} -mediated shortening of the ventricular action potential. In the basic framework discussed above, the first mechanism is explained by accelerated Ca uptake into the SR, resulting in a more rapid rate of recovery of RyR refractoriness (which is sensitive to both cytosolic and luminal Ca levels). At any given cycle length, this means that a greater proportion of RyRs are fully recovered in time for the next beat, which prevents oscillations in Ca release. Concomitantly, the Ca load of the SR will also recover more quickly, preventing oscillations of Ca load and release (as in Diaz et al.). Both mechanisms (or a combination) can adequately explain why SNS, and noradrenaline, act to suppress alternans, and is supported by our experimental observations, namely, the leftward shift in the APD and Ca alternans cycle length relationships and leftward shift in the Ca transient S1S2 (extra-stimulus) restitution curve. Indeed, there is already good evidence that SERCA is a critical regulator of alternans. For example, Cuttler et al. showed that targeted overexpression of genes for SERCA2a in isolated guinea pig myocytes and intact hearts acts to suppresses both Ca and APD alternans (Cutler et al., 2009). Similarly, Laurita et al. described regional heterogeneities in SERCA expression that correlate with the magnitude of alternans across the ventricular wall of the canine heart (Laurita et al., 2003). In the present study, pharmacological inhibition of SERCA exerted the opposite effect to that of SNS and noradrenaline, which indirectly supports the importance of altered SERCA activity in suppression of APD and Ca alternans during adrenergic stimulation.

The second mechanism by which adrenergic-stimulation suppresses APD alternans is through I_{Ks} -mediated shortening of the ventricular action potential. Two potential mechanisms could explain this observation. Firstly, the slope of the restitution curve is largely determined by the APD at steady-state (Shattock et al., 2017) and shortening of the action potential with SNS acts to flatten this relationship. Altered restitution kinetics, secondary to I_{Ks} -mediated action potential adaptation, could perceptibly dampen the magnitude of APD alternans. Notably, this does not require that the slope of the curve be >1 , as in the classical proposal of Nolasco and Dahlen (Nolasco and Dahlen, 1968). Rather, a shorter action potential is predicted to exhibit smaller alternans than an action potential of longer initial duration, simply because it is shorter in the first place. This is an inherent physical property of the action potential that arises from the non-linear dependence of APD on repolarisation rate (see Zaza, 2010;

Winter and Shattock, 2016). The potential second mechanism is that I_{Ks} -mediated shortening of the action potential may indirectly regulate intracellular Ca handling. It is known that the duration of the action potential influences cellular Ca influx and efflux, and prolonging the action potential results in an increase in Ca load and slowing in the rate of decay of the Ca transient (Bouchard et al., 1995). I_{Ks} -mediated shortening of the action potential may therefore enhance cytosolic Ca extrusion by limiting Ca entry via L-type Ca current and/or by modulating Ca flux through the sarcolemmal sodium-Ca exchanger.

The results of the present study differ from previous reports in the rabbit heart, which suggest that SNS leads to a steepening of the electrical restitution curve, an increase in the magnitude of APD alternans and a decrease in the ventricular fibrillation threshold (a pseudo-quantitative measure of susceptibility to ventricular fibrillation). However, we found that SNS acts to suppress APD alternans, in line with earlier reports on mechanical and T-wave alternans in dogs (Euler et al., 1996) and supported by several reports in isolated myocytes treated with sympathomimetic agents (Hüser et al., 2000; Florea and Blatter, 2012). Moreover, our findings are in keeping with more recent thinking on the primacy of Ca cycling instabilities as a driver for APD alternans. However, we cannot discount that the difference between our study and the study of Ng et al. reflect the species used (guinea pig vs. rabbit) or methodological differences between studies (optical mapping vs. monophasic action potential recordings). Notably, there are measurable differences in electrophysiology between experimental mammalian species, most markedly between smaller and larger species (rat/mouse vs. rabbit/dog), but the rabbit is also known to exhibit a distinct biphasic restitution relationship (Szigligeti et al., 1998). It is feasible that species-specific differences could account for the discord between the effects of SNS on alternans in rabbits and guinea pigs (and other species). Whether the results of our experiments in the guinea pig are generalizable to other species is not known and requires further study.

Study Limitations and Technical Discussion

This study has several limitations. Firstly, because we used Rhod-2, a single wavelength fluorescent indicator, the presented values for Ca transient alternans are only relative and cannot be reliably calibrated in the isolated heart. However, this is unlikely to impact on the main conclusions of the study. Furthermore, the use of uncoupling agents in optical mapping is a recognized technical limitation, with the potential to adversely affect cardiac electrophysiology (Brack et al., 2013). In the present study, we observed no obvious electrophysiological changes following blebbistatin perfusion in the guinea pig heart, in keeping with reports in other species (Fedorov et al., 2007).

In the present study, alternans were only observed at pacing cycle lengths shorter than 120 ms, which differs from the classical studies of Pastore et al., where alternans were observed in guinea pig hearts paced at slower rates (Pastore et al., 1999). This disparity most likely reflects that Pastore et al. performed

their studies at relatively cool temperatures (27°C vs. 37°C) and with lower buffer Ca than used presently (1.2 mmol/L vs. 1.6 mmol/L), both of which would prolong APD and so shift the alternans threshold to slower rates. In addition, to avoid sustained periods of nerve stimulation, which could cause rundown of nerve responses, we utilized a dynamic pacing protocol, whereas previous studies have used more sustained pacing periods (~1 min per cycle length).

CONCLUSION(S)

SNS suppresses APD and Ca alternans in the intact guinea pig heart by accelerated intracellular Ca handling and via I_{Ks} -mediated shortening of the ventricular action potential.

AUTHOR CONTRIBUTIONS

JW was responsible for the central hypothesis, design and implementation of the study, collection and analysis of most experimental data and primarily responsible for drafting of the manuscript. CW, MB, and MS contributed to the study design,

analysis of experimental data and drafting of the manuscript. CW also assisted with the collection and analysis of the experimental data. CO and DP provided expertise in the analysis of the optical mapping datasets, the interpretation of the results and drafting of the final manuscript.

FUNDING

JW (FS/16/35/31952) and MS (RG/12/4/29426) are supported by the British Heart Foundation. This work was also supported by the National Institute for Health Research Biomedical Research Centre at Guy's and St. Thomas' National Health Foundation Trust and King's College, in addition National to the Centre of Excellence in Medical Engineering funded by the Wellcome Trust and Engineering and Physical Sciences Research Council (EPSRC; WT 203148/Z/16/Z). The views expressed are those of the author(s) and not necessarily those of the National Health Service, the National Institute for Health Research, or the Department of Health. MB acknowledges the support of the UK Medical Research Council through a New Investigator Research Grant (MR/N011007/1).

REFERENCES

- Bers, D. M. (2002). Cardiac excitation-contraction coupling. *Nature* 415, 198–205. doi: 10.1038/415198a
- Bouchard, R. A., Clark, R. B., and Giles, W. R. (1995). Effects of action potential duration on excitation-contraction coupling in rat ventricular myocytes. Action potential voltage-clamp measurements. *Circ. Res.* 76, 790–801. doi: 10.1161/01.RES.76.5.790
- Brack, K. E., Narang, R., Winter, J., and Ng, G. A. (2013). The mechanical uncoupler blebbistatin is associated with significant electrophysiological effects in the isolated rabbit heart. *Exp. Physiol.* 98, 1009–1027. doi: 10.1113/expphysiol.2012.069369
- Cutler, M. J., Wan, X., Laurita, K. R., Hajjar, R. J., and Rosenbaum, D. S. (2009). Targeted SERCA2a gene expression identifies molecular mechanism and therapeutic target for arrhythmogenic cardiac alternans. *Circ. Arrhythm. Electrophys.* 2, 686–694. doi: 10.1161/CIRCEP.109.8.63118
- Díaz, M. E., O'Neill, S. C., and Eisner, D. A. (2004). Sarcoplasmic reticulum calcium content fluctuation is the key to cardiac alternans. *Circ. Res.* 94, 650–656. doi: 10.1161/01.RES.0000119923.64774.72
- Euler, D. E., Guo, H., and Olshansky, B. (1996). Sympathetic influences on electrical and mechanical alternans in the canine heart. *Cardiovasc. Res.* 32, 854–860. doi: 10.1016/S0008-6363(96)00151-4
- Fedorov, V. V., Lozinsky, I. T., Sosunov, E. A., Anyukhovskiy, E. P., Rosen, M. R., Balke, C. W., et al. (2007). Application of blebbistatin as an excitation-contraction uncoupler for electrophysiologic study of rat and rabbit hearts. *Heart Rhythm* 4, 619–626. doi: 10.1016/j.hrthm.2006.12.047
- Florea, S. M., and Blatter, L. A. (2012). Regulation of cardiac alternans by β -adrenergic signaling pathways. *Am. J. Physiol. Heart Circ. Physiol.* 303, H1047–H1056. doi: 10.1152/ajpheart.00384.2012
- Hüser, J., Wang, Y. G., Sheehan, K. A., Cifuentes, F., Lipsius, S. L., and Blatter, L. A. (2000). Functional coupling between glycolysis and excitation—contraction coupling underlies alternans in cat heart cells. *J. Physiol.* 524(Pt 3), 795–806. doi: 10.1111/j.1469-7793.2000.00795.x
- Laurita, K. R., Katra, R., Wible, B., Wan, X., and Koo, M. H. (2003). Transmural heterogeneity of calcium handling in canine. *Circ. Res.* 92, 668–675. doi: 10.1161/01.RES.0000062468.25308.27
- Ng, G. A., Brack, K. E., and Coote, J. H. (2001). Effects of direct sympathetic and vagus nerve stimulation on the physiology of the whole heart—a novel model of isolated Langendorff perfused rabbit heart with intact dual autonomic innervation. *Exp. Physiol.* 86, 319–329. doi: 10.1113/eph8602146
- Ng, G. A., Brack, K. E., Patel, V. H., and Coote, J. H. (2007). Autonomic modulation of electrical restitution, alternans and ventricular fibrillation initiation in the isolated heart. *Cardiovasc. Res.* 73, 750–760. doi: 10.1016/j.cardiores.2006.12.001
- Nolasco, J. B., and Dahlen, R. W. (1968). A graphic method for the study of alternation in cardiac action potentials. *J. Appl. Physiol.* 25, 191–196. doi: 10.1152/jappl.1968.25.2.191
- Pastore, J. M., Girouard, S. D., Laurita, K. R., Akar, F. G., and Rosenbaum, D. S. (1999). Mechanism linking T-wave alternans to the genesis of cardiac fibrillation. *Circulation* 99, 1385–1394. doi: 10.1161/01.CIR.99.1.0.1385
- Picht, E., DeSantiago, J., Blatter, L. A., and Bers, D. M. (2006). Cardiac alternans do not rely on diastolic sarcoplasmic reticulum calcium content fluctuations. *Circ. Res.* 99, 740–748. doi: 10.1161/01.RES.0000244002.88813.91
- Qu, Z., Liu, M. B., and Nivala, M. (2016). A unified theory of calcium alternans in ventricular myocytes. *Sci. Rep.* 6:35625. doi: 10.1038/srep35625
- Shattock, M. J., Park, K. C., Yang, H. Y., Lee, A. W. C., Niederer, S., MacLeod, K. T., et al. (2017). Restitution slope is principally determined by steady-state action potential duration. *Cardiovasc. Res.* 113, 817–828. doi: 10.1093/cvr/cvx063
- Shkryl, V. M., Maxwell, J. T., Domeier, T. L., and Blatter, L. A. (2012). Refractoriness of sarcoplasmic reticulum Ca^{2+} release determines Ca^{2+} alternans in atrial myocytes. *Am. J. Physiol. Heart Circ. Physiol.* 302, H2310–H2320. doi: 10.1152/ajpheart.00079.2012
- Szigligeti, P., Báýánsz, T., Magyar, J., Szigeti, G. Y., Papp, Z., Varró, A., et al. (1998). Intracellular calcium and electrical restitution in mammalian cells. *Acta. Physiol. Scand.* 163, 139–147. doi: 10.1046/j.1365-201X.1998.00362.x
- Wang, L., Myles, R. C., De Jesus, N. M., Ohlendorf, A. K. P., Bers, D. M., and Ripplinger, C. M. (2014). Optical mapping of sarcoplasmic reticulum Ca^{2+} in the intact heart. *Ryanodine Receptor Refractoriness During Alternans and Fibrillation. Circ. Res.* 114, 1410–1421. doi: 10.1161/CIRCRESAHA.114.302505
- Weiss, J. N., Nivala, M., Garfinkel, A., and Qu, Z. (2011). Alternans and arrhythmias: from cell to heart. *Circ. Res.* 108, 98–112. doi: 10.1161/CIRCRESAHA.110.223586

- Winter, J., and Shattock, M. J. (2016). Geometrical considerations in cardiac electrophysiology and arrhythmogenesis. *Europace* 18, 320–331. doi: 10.1093/europace/euv307
- Wu, Y., and Clusin, W. T. (1997). Calcium transient alternans in blood-perfused ischemic hearts: observations with fluorescent indicator Fura Red. *Am. J. Physiol. Heart Circ. Physiol.* 273, H2161–H2169. doi: 10.1152/ajpheart.1997.273.5.H2161
- Zaza, A. (2010). Control of the cardiac action potential: the role of repolarization dynamics. *J. Mol. Cell. Cardiol.* 48, 106–111. doi: 10.1016/j.yjmcc.2009.07.027

Conflict of Interest Statement: The authors declare that the research was conducted in the absence of any commercial or financial relationships that could be construed as a potential conflict of interest.

Copyright © 2018 Winter, Bishop, Wilder, O'Shea, Pavlovic and Shattock. This is an open-access article distributed under the terms of the Creative Commons Attribution License (CC BY). The use, distribution or reproduction in other forums is permitted, provided the original author(s) or licensor are credited and that the original publication in this journal is cited, in accordance with accepted academic practice. No use, distribution or reproduction is permitted which does not comply with these terms.